Proceedings of the Research Institute of Atmospherics,
Nagoya University, vol. 28(1981) –Research Report–

AN IMPROVED REAL-TIME WHISTLER ANALYZER USING A MICRO-COMPUTER SYSTEM

Ai-ichiro TSUZUKU, Toshimi OKADA and Akira IWAI

Abstract

In order to measure precisely the dispersion of whistlers, the $\rho-\theta$ transformation method and the templet matching method were tested. It has been shown from computer simulations that both the methods are effective for precise measurements of whistler dispersion and the latter is better to realize an apparatus for real-time measurements of whistler dispersion. On the basis of templet matching method, we have realized an improved real-time whistler analyzer. In this report, we describe the principle of the dispersion analysis and the performance of the improved apparatus.

1. Introduction

Energy from a lightning discharge enters the ionosphere and is guided by the lines of force of the earth's magnetic field into the opposite hemisphere.[1] As the radio waves travel along this path, they are dispersed. Whistlers are these dispersed signals at very low frequency (VLF) that "whistle". Their dispersions depend on the electron density and the magnitude of the earth's magnetic field along their propagation path; thus, precise measurements of whistler dispersion enable us to investigate the electron density profile in the ionosphere and the magnetosphere.[2]

Routine-based observations of whistlers have usually been carried out by two-minute magnetic-tape recording every hour. The aural detection has been made for identifying whistlers, and whistler dispersions are measured on the frequency-time spectrograms represented by a sound spectrograph.

In order to reduce the load of this bothering work, an real-time whistler analyzer has recently been developed and it has been shown that the analyzer is very effective for the identification of whistlers and for the measurement of the dispersions of discrete-pure type whistlers,[3] but it is required to be improved to measure precisely the dispersion of multi-flash type whistlers and diffused ones.

In this report, we show newly developed methods for the whistler signal analysis which are considerably effective in measuring the dispersions of whistlers of diffused type as well as of discrete-pure type.

2. Principle of the Signal Analysis

2-1 f to s transformation

The frequency-time spectra of whistlers are shown in Fig.1. As is seen from Fig.1, the whistler is a kind of frequency-modulated signal whose frequency decreases with time, according to the following relation of

$$f=D^2/t^2 , \tag{1}$$

where f is the wave frequency and t is the propagation time measured from the causative atmospheric. D is the dispersion constant.

Now we replace the value of the frequency axis 'f' by 's', which is related to f as follows,

$$S=f^{-\frac{1}{2}}, \tag{2}$$

so the equation (1) becomes ,

$$S=\frac{1}{D}\cdot t \ . \tag{3}$$

When the VLF signals are displayed on the s-t domain, a whistler is depicted as a straight line, which is shown in Fig.2. If we can measure the inclination of the straight line, we can get the

dispersion by the relation of eq.(3).

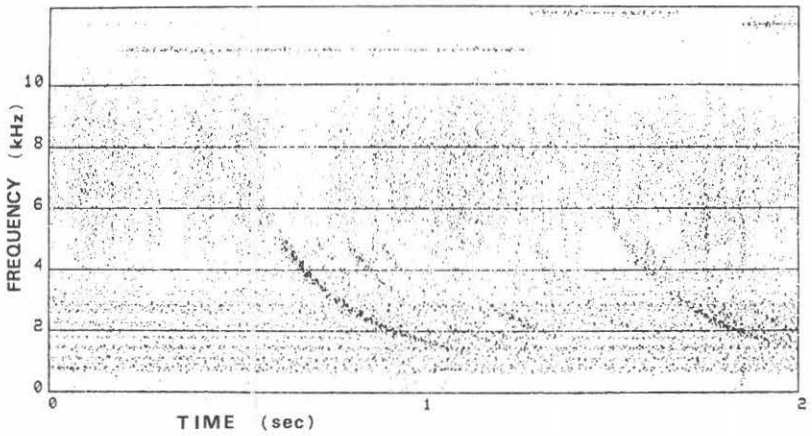

Fig.1 Dynamic spectra of whistlers on the frequency-time(f-t) diagram.

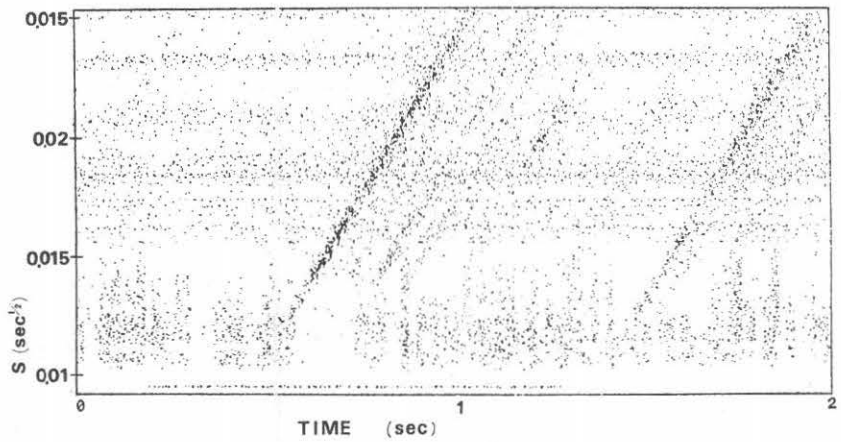

Fig.2 Transformed spectra of whistlers represented in Fig.1 on the S-t diagram, where s is given by $S=1/\sqrt{f}$.

We examined the following two methods to measure the inclination of the straight line on the s-t domain: the $\rho-\theta$ transformation method and the templet matching method. To evaluate these two methods, we first tested their effectiveness by use of computer simulations. Fig.3 indicates the block diagram of the signal flow in our computer simulation system. The whistler signals on the magnetic tapes and the pseudo-whistlers generated by the pseudo-whistler generator are fed to

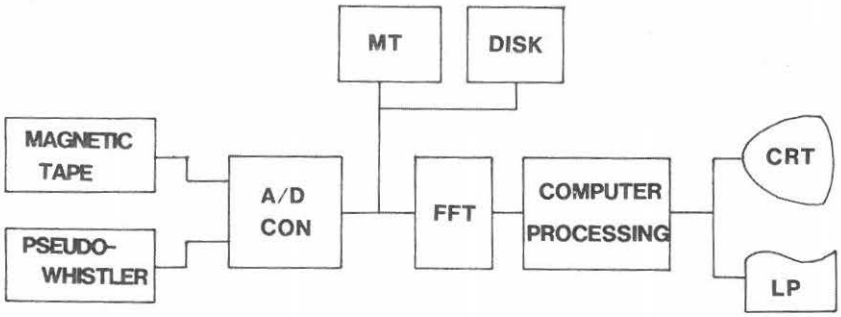

Fig.3 Block diagram of the simulation system of whistlers by use of the computer.

the Analog-to-Digital converter(A/D) to be encoded in the digital form in a sampling frequency of 25kHz. The encoded data are stored on the magnetic tapes(MT) or the disc memory(DISK). Then, these signals are analyzed by the following two methods. The obtained results are displayed on the cathode ray tube(CRT) or the line printer(LP). The pseudo-whistler generator will be explained in the appendix.

2-2 $\rho - \theta$ transformation method

$\rho - \theta$ transformation is one of the coordinate transformations. The principle of this transformation is shown in Fig.4. Assume that there

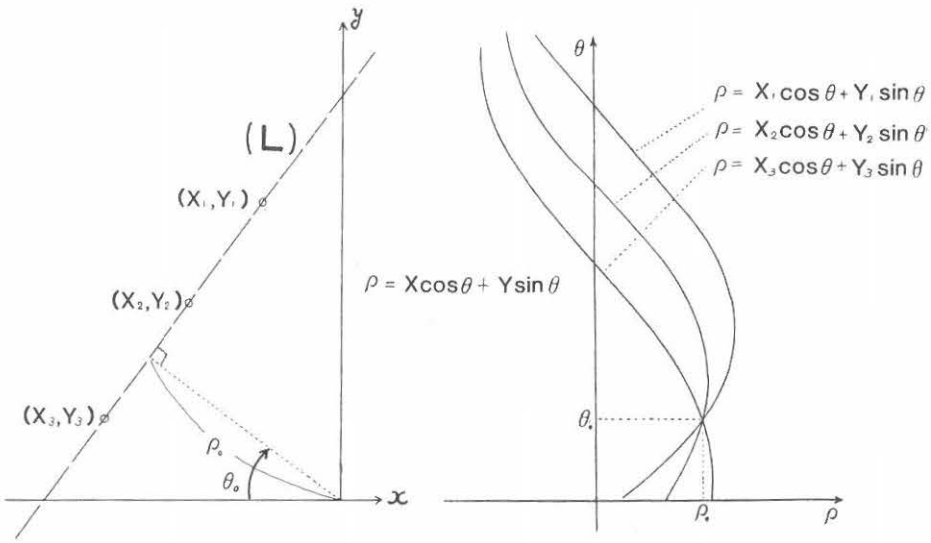

Fig.4 Schematic diagram of coordinate transformation from x-y domain to $\rho - \theta$ domain.

are a straight line (L) in the x-y coordinate and the points P_i (x_i, y_i) $(i=1,2,\cdots,n)$ on the line. The line is uniquely defined by the orthogonal line whose length from the origin(0,0) is ρ_0 and the angle measured clockwise from x axis is θ_0 . Next we introduce the $\rho-\theta$ coordinate system. A point in the x-y coordinate system is projected on the $\rho-\theta$ coordinate as a sinusoidal curve through the relation

$$\rho = x_i \cos\theta + y_i \sin\theta \quad . \tag{4}$$

For example, three points on the same straight line in the x-y coordinate system are transformed into three different curves, as is shown in Fig.4. The noticeable characteristics of the curves in the $\rho-\theta$ coordinate are that all the curves intersect at one point (ρ_0, θ_0). If the points are not on the same line, the intersection does not occur at a certain point on the $\rho-\theta$ plane.

Therefore, in order to measure the dispersion of whistlers, we detect the existence of the intersection mentioned above and then measure the value θ of the point of the intersection.

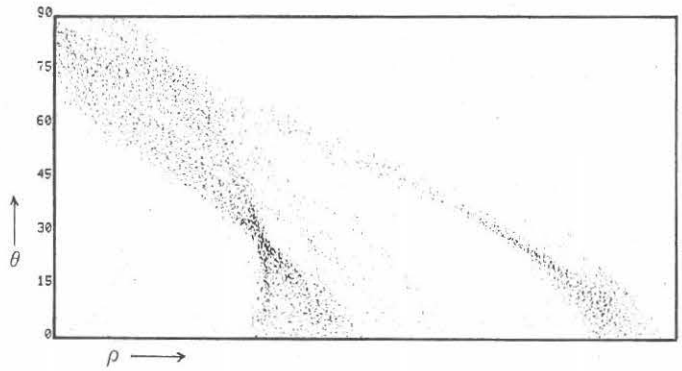

Fig.5 Transformed patterns on the $\rho-\theta$ coordinate for whistlers represented in Fig.2.

An example of the $\rho-\theta$ transformation is shown in Fig.5, corresponding to the data in the x-y coordinate in Fig.2. From Fig.5 we can find the intersection at $\theta=27^\circ$ which corresponds to D=30 $(\sec^{1/2})$. The direct measurement of the dispersion from the f-t diagram shown in Fig.1 also gives the same dispersion(D=30). So we can conclude that the $\rho-\theta$ transformation method is effective for the measurement of the dispersion.

The inclination of impulsive noises such as atmospherics is parallel to the y axis(i.e. 90 degrees), so that the intersection on

the $\rho-\theta$ plane should occurr at $\theta=0^{\circ}$. While, whistlers of the dispersion ranging 10-80 ($sec^{1/2}$) intersect between $\theta=10^{\circ}$ and 70°. From this difference, it is easily accomplished to distinguish impulsive noises from whistlers.

2-3 Templet matching method

As was mentioned in section (2-1), the dispersion of whistlers is given by the inclination of the straight line in the s-t domain. The templet matching method is used to measure directly the inclination of the line. The templets mean the standard straight lines whose inclinations are calibrated to coincide with the whistler dispersions (D=10-80).

The process of the templet matching is illustrated in Fig.6. The solid lines in Fig.6-a show the five templets with the different dispersions of 20,30,40,60 and 80 ($sec^{1/2}$), whose origins are on the

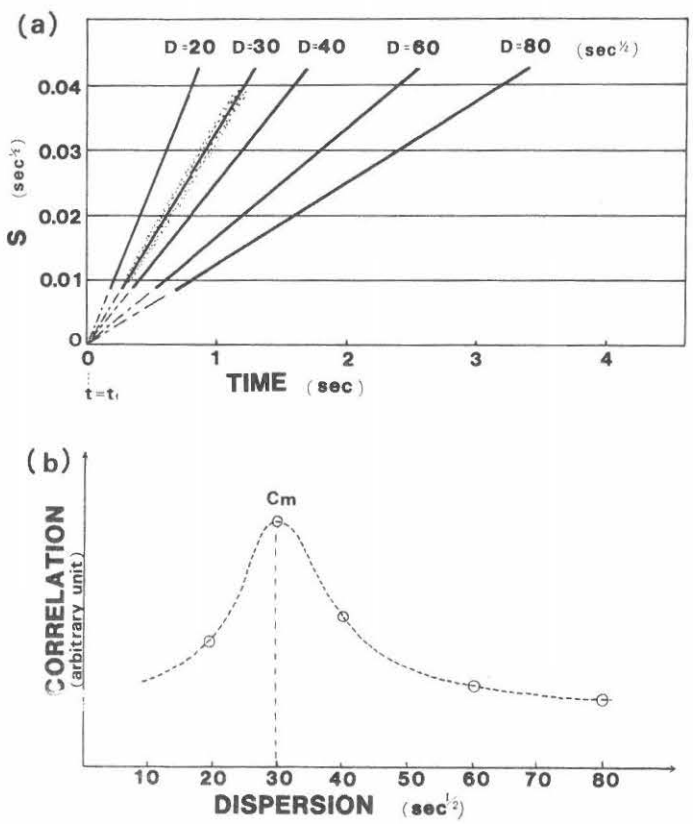

Fig.6 Schematic diagram showing the process of the templet matching.
(a) The straight lines indicate the templets originating at a specific time of $t=t_1$ with their dispersion of 20 to 80 ($sec^{1/2}$). dots along the straight line of D=30 ($sec^{1/2}$) refer to a whistler.
(b) correlation values calculated among the templets in the panel (a) and the whistler. They amount to a maximum (Cm) at D=30 ($sec^{1/2}$).

same point P(t=t_1,s=0). The dots distributed along a certain templet (D=30) correspond to a whistler. In this example, the dispersion of the whistler is 30 ($sec^{1/2}$) and its origin is also on the same point as for the templets. Fig.6-b shows a schematic diagram of correlations among the dotted curves for the whistler and a group of templets with various dispersions, where the correlation value reaches a maximum at D=30. The principle to obtain the above correlations will be shown in Fig.9.

When impulsive noises distributed around the templet of D=0 such as atmospherics are received, there appear comparatively small correlations among impulsiv noises and the templets with the different dispersions, but no induced correlations interfer in the measurements of whistler dipersion, as will be shown in Fig.11.

2-4 Comparison between the two analysis methods

We have compared these two analysis methods from the standing point of 'computing time' to estimate the dispersion. Let's consider the case when VLF signals with their duration of 2 seconds are analyzed by use of these two methods. This duration is long enough to contain a whistler with its frequency range of 1.6-10 kHz, and its dispersions of from 10 to 80 ($sec^{1/2}$). In the ρ-θ transformation method, the computing time to execute the caluculation expressed in eq.(4) is estimated as follows.

When we intend to measure the dispersion ranging 10-80 ($sec^{1/2}$) with the mesuring step of 1 ($sec^{1/2}$), it is needed to divide the data on the x-y coordinate into 10,000 segments (100 x components, 100 y components). For one of the segments, ρ is caluculated against the ranging from 10 to 70 degrees with the step of 1 degree. For a selected segment (x_i,y_i) and a particular angle θ, eq.(4) requires 2 times the calculation of a sinusoidal function; multiplications and an addition. Consequently, the whole process to measure the dispersion needs at least 1,220,000 (100×100×61×2) times the multiplication.

On the contrary, in the templet matching method, only 100 times additions are needed to match between VLF signals on the x-y coordinate system and a templet with a particular dispersion. Therefore, when we intend to match between VLF signals and a bundle of templets of D=10 to 80 ($sec^{1/2}$) with the step of 1 ($sec^{1/2}$), 810,000 times additions should be needed. The process of addition is more quickly executed than that of multiplication by the computer. Considering these facts, we can conclude that the templet matching method is

better for an equipment using the micro-processor.

The above-mentioned less computing time leads us to adopt the templet matching method for the real-time whistler analyzer.

3. Real-time Whistler Analyzer

Here we show the specification of the equipment for the measurement of whistler dispersion based on the templet matching method.

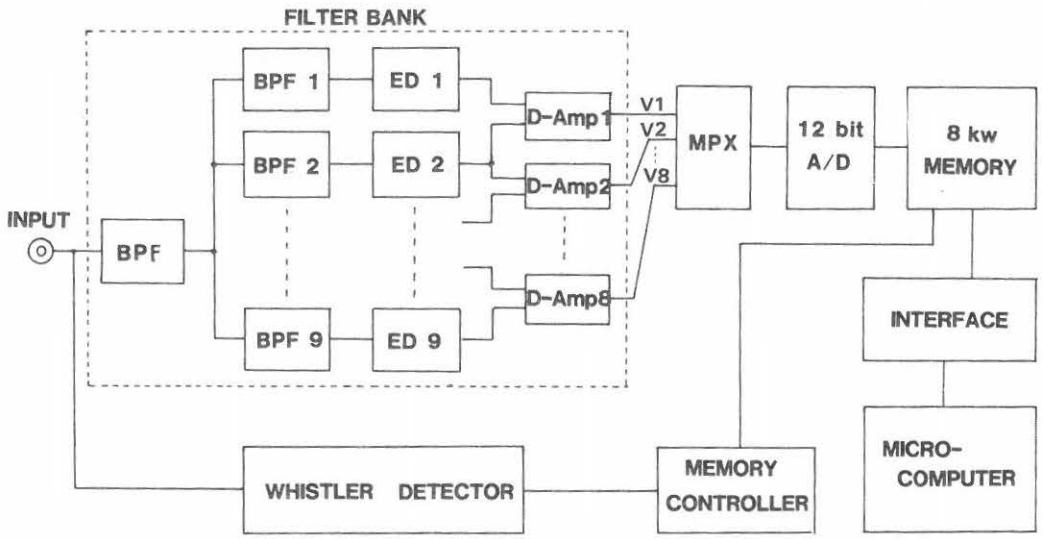

Fig.7 Block diagram of the improved real-time whistler analyzer based on the templet matching method.

The block diagram of the equipment is shown in Fig.7. The equipment consists of a filter bank, a whistler detector, an analog to digital converter with an 8-line-to-1-line data multiplexer(MPX), a static memory and a micro-processor. The filter bank is composed of a wide band pass filter(BPF), nine narrow band pass filters(BPF), nine envelope detectors(ED) and eight differential amplifiers(D-amp). The specific frequencies of the narrow band pass filters are chosen according to the three criterions given by OKADA et al.[3], and the relation among the frequencies of the nine filters is as follows,

$$T=D\cdot(f_K^{-\frac{1}{2}}-f_{K+1}^{-\frac{1}{2}}) \qquad (5)$$

where $f_k (f_k < f_{k+1})$ is the frerquency of the k-th filter.

The output signals from ED-1 and ED-2 are differentially amplified, resulting in a differential output V_1. Similarly the signals $V_2, V_3, \cdots, V_8$ are obtained. An example of these eight outputs is shown in Fig.8. In this case the dispersion is 40 ($sec^{1/2}$). It is seen in Fig.8 that each of the output signals $V_1, V_2, \cdots, V_8$ shows a sinusoidal oscillation and that the time differences between the adjacent two outputs are equal. The inclination of a straight line referring to these constant time differences gives the dispersion of the whistler.

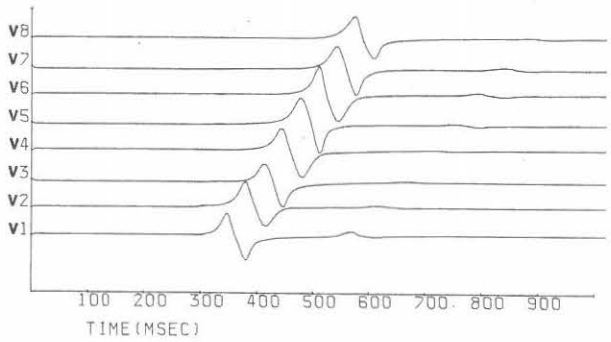

Fig.8 Wave forms of the signalg from the filter bank corresponding to a puseudo-whistler with its dispersion of 40 ($sec^{1/2}$).

Next the output signals from the eight D-amps are sampled and converted into the binary digital mode by the A/D converter to be recorded on the static memory with a capacity of 8 kilo-words.

The control to start and stop the data-recording from the A/D converter to the static memory is made by the memory-controller. It generates command signals when a whistler is identified by the whistler-detector. The process of the whistler identification has been already described in detail by OKADA et al.[3] and OKADA.[4]

The dispersion range of whistlers which are usually observed at low latitudes such as Moshiri (geomag.lat. 34° N) is from 15 to 80 ($sec^{1/2}$); thus, the longest time difference between the signals V_1 and V_8 is estimated to be 500(msec) from eq.(5). The output signals $V_1, V_2, \cdots$ and V_8 are recorded on the static memory in such a way that these signals like a cycle of the sinusoidal oscillations are stored around the center of the address of the memory not to exclude the necessary data, by means of the function of the whistler detector and the memory-controller. The data recorded on the memory are transfered to the registers in the micro-processor, and the calculation of the dispersion of whistlers starts immediately.

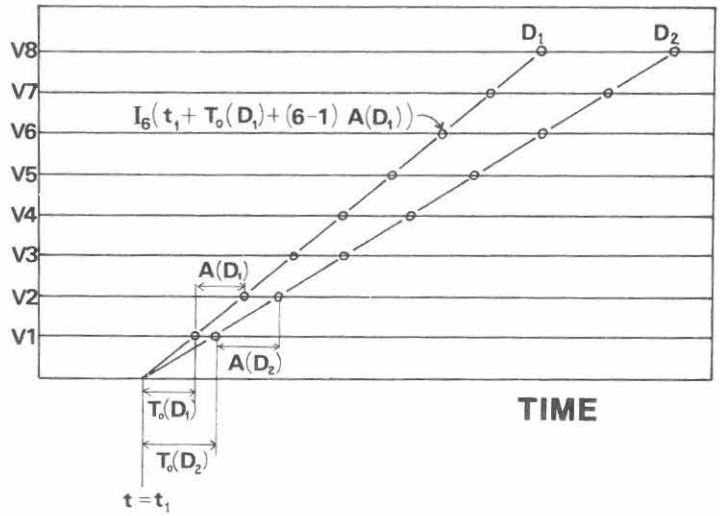

Fig.9 Illustration showing how to sum up the correlated intensities among a whistler and the templets with the same temporal origin of $t=t_1$, according to eq.(6).

Fig.9 is a schmatic diagram which shows how to evaluate the degree of the templet matching. The evaluation is made by summing up the eight output intensities($I_j, j=1,2,\cdots,8$) that match the templet with a certain dispersion, for instance, D1. The summation (C) is written as

$$C(t,D)=\sum_{j=1}^{8} I_j(t+T_0(D)+(j-1)\cdot A(D)) \quad , \tag{6}$$

where t is the time of the starting point of the matching and D is the dispersion of whistler. T (D) is the bias of time with which the summation expressed in eq.(6) starts at V_1. $I_j(t)$ is the intensity of the output signal from the j-th differential amplifier in the filter bank. A(D) is a temporal segment interval which depends on the dispersion of whistler and is given by

$$A(D)=\frac{1}{9}\left(f_{min}^{-\frac{1}{2}}-f_{max}^{-\frac{1}{2}}\right) \quad . \tag{7}$$

The above-mentioned summation is first executed along the straight line that corresponds to the dispersion of 10 ($sec^{1/2}$) and intersects the abscissa of the time axis at a specific time of $t=t_1$, and subsequently the summations are made along the straight lines with the same intersecting time (t_1) until the dispersions for the lines reach 80 ($sec^{1/2}$) by a dispersion step of D=1 ($sec^{1/2}$). Then the similar summations are repeated for each of the intersecting times given by

$$t=t_1+N\Delta t \quad (N=1,2,\cdots,N_{max}) \ , \tag{8}$$

$$\Delta t=T/N_{max} \ , \tag{9}$$

where T is the whole duration when the summations are performed and N_{max} is the repeating number for the summations. In our case, T is chosen to be 50 (msec), and N_{max}=10.

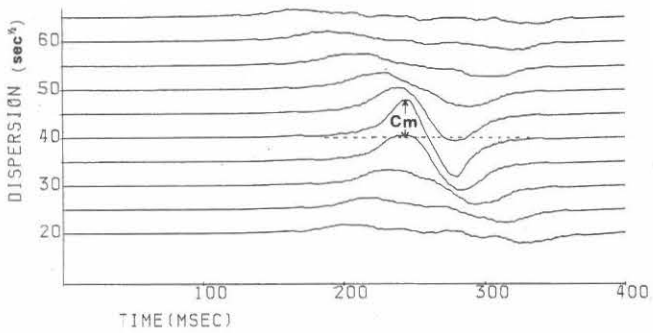

Fig.10 Summed up intensities correlated among the whistler shown in Fig.8 and the templets with their dispersions 20 to 70 (sec$^{1/2}$). The intensities show a maximum (Cm) at D=40 (sec$^{1/2}$).

Fig.10 shows an example of the obtained results of the data summation. The input signal is the same as for Fig.8. The ordinate is for the dispersion of the templet and the abscissa for the starting time of the matching. It is clearly seen that the matching intensity given by eq.(6) depends both on the dispersion of the templet and on the starting time of the matching. When we examine the dependence of the matched intensity on the time for a specific value of the templet dispersion, there are generally two maxima in opposite senses; positive and negative. This can be easily explained by the fact that the output signals from the differential amplifiers are first shifted positive and negative after a short time , when a whistler is received , as is seen from Fig.8.

Correspondingly, the summation of all the output signals executed with a specific time difference given in eq.(6) shows a characteristic pattern; a positive maximum and a subsequent negative maximum.

The dispersion of whistler is measured by detecting the maximum value Cm. The dispersion of the templet for the maximum Cm is the dispersion of the received whistler. The experiment using the pseudo-whistler generator confirms the measuring accuracy of dispersion less than ±1 (sec$^{1/2}$) for the whistler dispersion ranging D=10-80 (sec$^{1/2}$).

Finally, we show an example of the response of our whistler analyzer for whistlers observed st Sakushima(geomag.lat. 24° N).

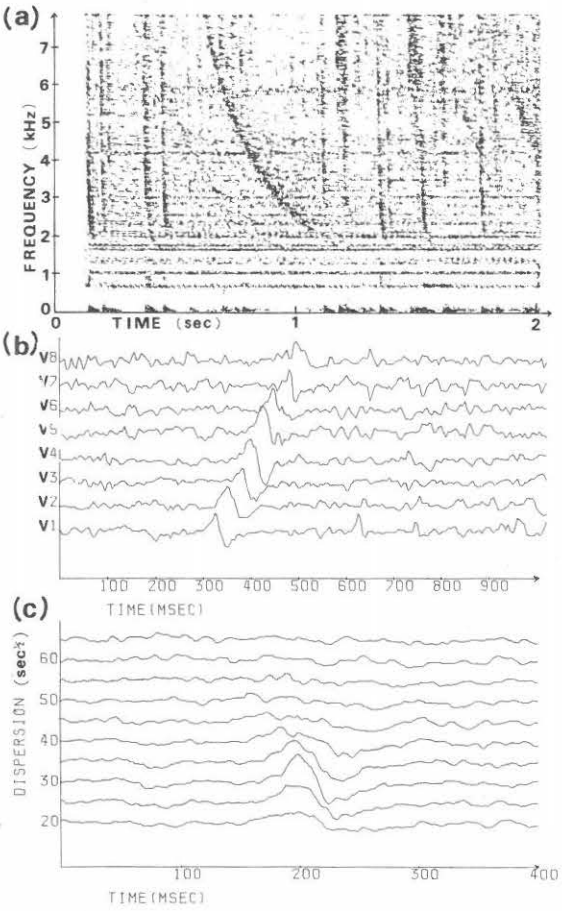

Fig.11 (a) The dynamic spectra of the whistlers observed at Sakushima(geomag.lat.24° N). (b) The response of the filter bank relevant to the whistlers in the panel (a). (c) The correlated intensities from the templet matching.

Fig.11-a shows the dynamic spectrum of a whistler immersed in various natural noises. Fig.11-b is the response of the filter bank. It is seen that the detector is more sensitive to the whistler than for other noises. The correlation shows a maximum at the templet of D=30 ($sec^{1/2}$), as is seen in Fig.11-c. The same value of 30 ($sec^{1/2}$) is confirmed on the sonagram; thus, it is concluded that the templet matching method is efficient for measuring the dispersion of natural whistlers.

4. Analysis of Diffused Whistlers and Multi-flash Ones

In the previous section (3) it has been shown that the dispersion of pure-discrete whistlers is automatically measured with a measuring accuracy less than ± 1 ($sec^{1/2}$). Now let's see the measurement of the dispersion of whistlers of the other types: diffused whistlers and multi-flash ones.

Fig.12

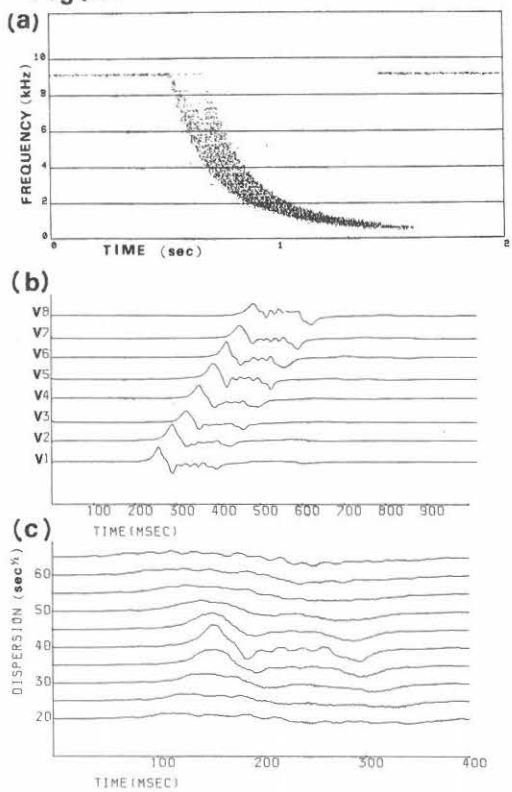

Fig.13

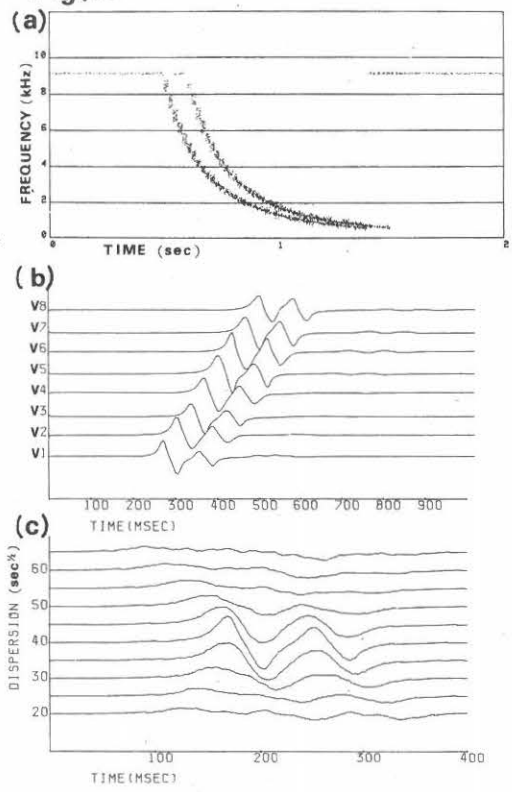

Fig.12 (a) The dynamic spectrum of a diffused whistler from the pseudo-whistler generator.
(b) The response of the filter bank relevant to the pseudo-whistler in the panel (a).
(c) The correlated intensities from the templet matching.

Fig.13 (a) The dynamic spectrum of two pseudo-whistlers whose time separation is small (80 msec).
(b) The response of the filter bank relevant to the pseudo-whistlers in the panel (a).
(c) The correlated intensities from the templet matching.

Fig.12-a shows the dynamic spectrum of a diffused whistler from the pseudo-whistler generator. Diffused whistlers are often observed at high and middle latitudes. The response of the filter bank relevant to the whistler is shown in Fig.12-b, where the output waveforms from the filter bank are considerably deformed than those for a pure whistler represented in Fig.8. But the correlation values among the outputs of V_1 to V_8 and the templets reach a maximum at t=160 (msec) and the templet of D=40 ($sec^{1/2}$) , resulting in deciding the dispersion of 40 ($sec^{1/2}$) for the diffused whistler.

Next, the time resolution of the equipment is examined. Fig.13-a shows the dynamic spectra of two pseudo-whistlers whose time separation is 80 (msec),and dispersions are both 40 ($sec^{1/2}$). In this case the response of the detector is so rapid that there occur double peaks , as shown in Fig.13-b, each of which corresponds to each of the multi-flash whistlers. And then the correlation values in Fig.13-c also indicate the corresponding double peaks at the templet of D=40 ($sec^{1/2}$). The time resolution of this analyzer is chosen to fix successive whistlers whose time separation is greater than 40 (msec).

5. Comparison Among the Three Analyzing Methods of Whistlers

In order to elucidate the effectiveness of the templet matching method, the comparative characteristics are represented in Fig.14 and Table 1 among the three analyzing methods of whistlers: the templet matching method, the $\rho-\theta$ transformation method and the real-time whistler analyzing by use of the cross-correlation between the outputs from the frequency discriminator.[3],[4] Fig.14 shows typical examples of the responses of the above three analyzers concerning three types of pseudo-whistlers: pure-discrete, multi-flash and diffused whistlers. The comparative performances among the above three methods are summarized in Table 1.

6. Concluding Remarks

As is seen in Table 1, the whistler analyzer with a

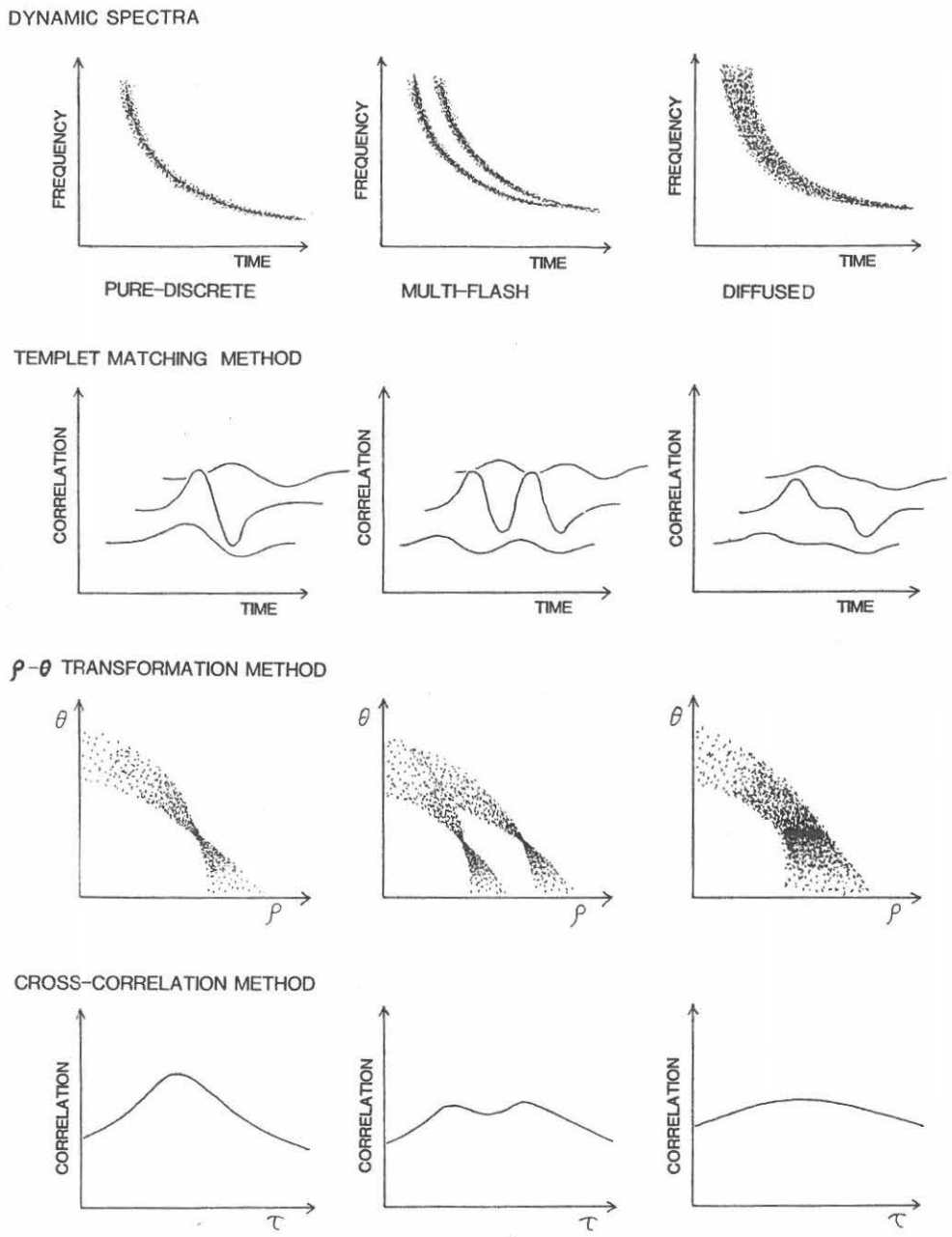

Fig.14 Comparative response patterns among the whistler analyzers based on the three methods (templet matching, ρ-θ transformation and cross-correlated methods) to measure the dispersion of three types of pseudo-whistlers; pure-discrete, multi-flash and diffused whistlers.

	Cross-correlation m.	ρ-θ transformation m.	Templet matching m.
Measuring range of the dispersion ($sec^{\frac{1}{2}}$)	10-85	10-80	10-80
Measuring accuracy ($sec^{\frac{1}{2}}$)	5	1	1
Time resolution (msec)	70	40	40
Interference of noises	medium	small	small
Measurements of the dispersion of the diffuse whistlers	difficult	capable	capable
Real-time measurement of the dispersion	in operation	difficult	to be realized

Table 1 Comparative performances among the three analyzing methods of whistlers.

micro-processor based on the templet matching is the most efficient to measure the dispersion of whistlers, and is of great use in studying the propagation characteristics of whistlers in the ionosphere and the magnetosphere. However, the present apparatus needs about one second to complete the calculation of the dispersion of a whistler, some improvements are required to reduce this calculating time.

Acknowledgment

The authors wish to express their sincere thanks to Dr. Y. Tanaka, Prof. J. Ohtsu and Dr. M. Hayakawa of their institute for their valuable discussion.

Appendix Pseudo-whistler Generator

We describe a pseudo-whistler generator which gives rise to signals just like the natural whistlers and is a greatly useful tool to calibrate the whistler analyzer. The frequency of the signal decreases according to the Eckersley's law, $D=t\sqrt{f}$, where f is the wave frequency and t is the time . Our pseudo-whistler generator has an advantage to generate diffused whistlers and multi-flash whistlers as well as pure-discrete ones.

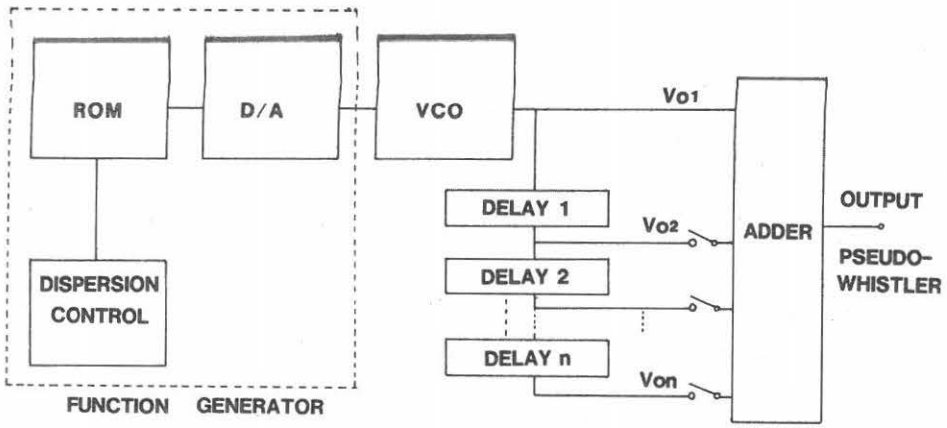

Fig.A-1 Block diagram of the pseudo whistler generator.

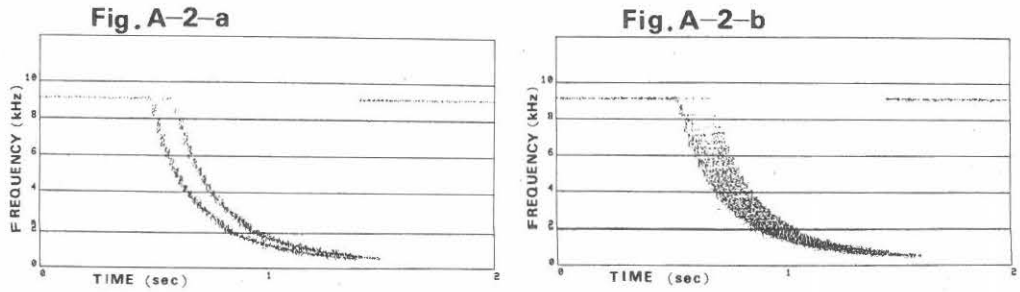

Fig.A-2-a The spectra of the pseudo multi-flash whistlers.
Fig.A-2-b The spectrum of the pseudo diffused whistler.

Fig.A-1 indicates the block diagram of the pseudo-whistler generator. It consists of a function generator, a voltage-controlled oscillator, a signal delay and an adder. The function generator gives

rise to a DC voltage function which varies with time according to the relation, $V=D^2/t^2$. As the function is memorized in the read-only-memory(ROM) , the changing speed of the voltage can be controlled by changing the speed of data-reading on ROM. The higher speed of data-reading corresponds to the smaller dispersion and vice-versa. The voltage from the function generator is fed to the voltage-controlled oscillator(VCO) whose output frequency is proportional to the input voltage; hence, the output signal from VCO can simulate a pure-discrete whistler , as shown in Fig.8. In addition, there are the multi-stages of the delay circuitsusing bucket burigade devices(BBD), which make a time delay of 20 (msec) per one block.When the original pseudo-whistler V_{01} from the VCO is added to one of the delayed signals from the BBD, the signals appear the multi-flash whistlers shown in Fig.A-2-a. Finally, the pseudo-diffused whistler is generated by adding many pure-discrete whistlers from the multi-stages of BBD, each time separation of which is very short. An example of the simulated diffused whistlers is shown in Fig.A-2-b.

References

(1) Storey L.O.R.: An investigation of whistling atmospherics, Phil.Trans.Roy.Soc., A246,113(1953).

(2) Helliwell R.A.: Whistlers and related ionospheric phenomena, Stanford University Press(1965).

(3) Okada T.,A. Iwai, J. Ohtsu and M. Satho: A real-time whistler analyzer, Proc. Res. Inst. Atmospherics, Nagoya Univ., 24,1 (1977).

(4) Okada T.: Study of low-latitude whistlers by the coordinated system of the direction finder and the real time whistler analyzer, Doctoral thesis, Nagoya Univ., (1980).